



ELSEVIER

Journal of Photochemistry and Photobiology A: Chemistry 121 (1999) 43–48

---

---

Journal of  
Photochemistry  
and  
Photobiology  
A: Chemistry

---

---

# Sensitized luminescence of the $\text{Eu}^{3+}/\text{La}^{3+}$ /cinnamic acid mixed complex: comparison to the $\text{Eu}^{3+}/\text{Gd}^{3+}$ /cinnamic acid mixed complex

János Erostyák\*, Andrea Buzády, István Hornyák, László Kozma

*Janus Pannonius University, Department of Experimental Physics, Ifjúság u. 6, Pécs H-7624, Hungary*

Received 22 June 1998; received in revised form 23 October 1998; accepted 12 November 1998

---

## Abstract

The photoluminescence properties of europium and lanthanum mixed complexes with cinnamic acid are described. The maximum emission intensity is found to be at about 80%  $\text{Eu}^{3+}$ /20%  $\text{La}^{3+}$  content at room temperature. The roles of intramolecular and intermolecular energy transfer processes are discussed. Comparison to photoluminescence properties of  $\text{Eu}^{3+}/\text{Gd}^{3+}$ /cinnamic acid mixed complexes is given. A slight photochemical degradation of the samples is found, the degree of which depends on the  $\text{Eu}^{3+}/\text{La}^{3+}$  ratio. © 1999 Elsevier Science S.A. All rights reserved.

*Keywords:* Intramolecular and intermolecular energy transfer; Sensitized luminescence of  $\text{Eu}^{3+}$ ; Time-resolved luminescence; Photochemical degradation

---

## 1. Introduction

Although the sensitized emission of lanthanide chelates was first observed in 1942 [1], they are still in the front of investigation and development. They are widely used in different fields, especially as luminescent labels in fluor-immunoassays [2–8]. Their application base on the energy transfer from the light absorbing ligands towards the central lanthanide ion [9–12].

In a previous work [13] we presented the interesting luminescence features of mixed complexes of europium and gadolinium with cinnamic acid ( $\text{Eu}/\text{Gd}/\text{CA}$ ). It was concluded that the luminescence properties of the samples studied in powder form are determined by both intra-, and intermolecular energy transfer processes (IntraMET and InterMET). In this highly luminescent material the so-called co-luminescent effect can be found, which means that the final emitter  $\text{Eu}^{3+}$  ions are pumped not only from cinnamic acids (CAs) bonded to these ions, but from CAs bonded to  $\text{Gd}^{3+}$  ions, too.

In this paper the luminescence properties of mixed complexes of  $\text{Eu}^{3+}/(\text{CA})_3$  and  $\text{La}^{3+}/(\text{CA})_3$  – (let  $\text{Eu}/\text{La}/\text{CA}$  stand for them) – are reported. The results shown below are very similar to those which were found in the case of  $\text{Eu}/\text{Gd}/\text{CA}$ .

A comparison between the two systems is also presented and the significant differences are discussed.

## 2. Experimental

The CA was first neutralized by NaOH, then the aqueous solution of  $\text{Eu}(\text{NO}_3)_3 \cdot 6\text{H}_2\text{O}$  and  $\text{La}(\text{NO}_3)_3 \cdot 6\text{H}_2\text{O}$  were added into CA solution. The mole ratio of lanthanides and CA was 1 : 3. A white precipitate was obtained, which was filtered and washed by double distilled water, then dried in vacuum at 80°C. A series of mixed complexes was prepared in which the  $\text{Eu}^{3+}$  content was gradually decreased and the  $\text{La}^{3+}$  content was increased. The materials were used in powder form for the measurements. Their chemical formulas are listed in Table 1.

The luminescence measurements (emission and excitation spectra, decay curves) were carried out by a PERKIN-ELMER LS50B luminescence spectrometer at room temperature using the solid sample holder. The spectrometer has a Xe flash lamp as excitation source. The time resolution of the instrument is 10  $\mu\text{s}$ . The spectra were measured in phosphorescence mode with an integrating gate of 5 ms which is long enough to integrate all the signals after the excitations. To determine the decay times the decay curves were measured in 10  $\mu\text{s}$  steps, which gives an excellent resolution in the case of sub-ms decays. The  $I_0$  initial intensities (see 3.3) were measured in fluorescence mode with an integrating gate of 10  $\mu\text{s}$ .

---

\*Corresponding author. Tel.: +36-72-327622/4399; fax: +36-72-501528; e-mail: erostyak@fizika.jpte.hu

Table 1  
Chemical formulas of mixed complexes of Eu/CA and La/CA

Serial number	Chemical formula
1	(C <sub>6</sub> H <sub>5</sub> CH=CHCOO) <sub>3</sub> (Eu <sub>1,0</sub> La <sub>0,0</sub> )
2	(C <sub>6</sub> H <sub>5</sub> CH=CHCOO) <sub>3</sub> (Eu <sub>0,9</sub> La <sub>0,1</sub> )
3	(C <sub>6</sub> H <sub>5</sub> CH=CHCOO) <sub>3</sub> (Eu <sub>0,8</sub> La <sub>0,2</sub> )
4	(C <sub>6</sub> H <sub>5</sub> CH=CHCOO) <sub>3</sub> (Eu <sub>0,7</sub> La <sub>0,3</sub> )
5	(C <sub>6</sub> H <sub>5</sub> CH=CHCOO) <sub>3</sub> (Eu <sub>0,6</sub> La <sub>0,4</sub> )
6	(C <sub>6</sub> H <sub>5</sub> CH=CHCOO) <sub>3</sub> (Eu <sub>0,5</sub> La <sub>0,5</sub> )
7	(C <sub>6</sub> H <sub>5</sub> CH=CHCOO) <sub>3</sub> (Eu <sub>0,4</sub> La <sub>0,6</sub> )
8	(C <sub>6</sub> H <sub>5</sub> CH=CHCOO) <sub>3</sub> (Eu <sub>0,3</sub> La <sub>0,7</sub> )
9	(C <sub>6</sub> H <sub>5</sub> CH=CHCOO) <sub>3</sub> (Eu <sub>0,2</sub> La <sub>0,8</sub> )
10	(C <sub>6</sub> H <sub>5</sub> CH=CHCOO) <sub>3</sub> (Eu <sub>0,1</sub> La <sub>0,9</sub> )
11	(C <sub>6</sub> H <sub>5</sub> CH=CHCOO) <sub>3</sub> (Eu <sub>0,0</sub> La <sub>1,0</sub> )

### 3. Results and discussion

#### 3.1. Excitation and emission spectra

The excitation (Fig. 1) and emission spectra (Fig. 2) of Eu/La/CA are very similar to the corresponding spectra of Eu/Gd/CA [13]. The excitation bands of the ligand and the Eu<sup>3+</sup> can be well identified (Fig. 1).

The ligand bands are centred at 240 and 335 nm. The slope over 370 nm is typical for powder samples and is believed to originate mainly from the non-monomer forms of the complexes. The La<sup>3+</sup> ions do not take part in the energy transfer processes. The Eu<sup>3+</sup> ions can be excited to

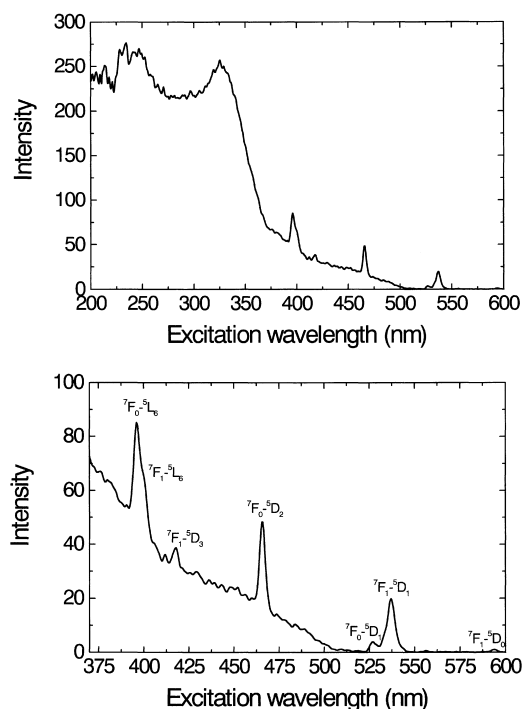


Fig. 1. Excitation spectrum of Eu/La/CA mixed complex.  $\lambda_{em} = 616$  nm. 80% Eu<sup>3+</sup>, 20% La<sup>3+</sup>. Initial sample.

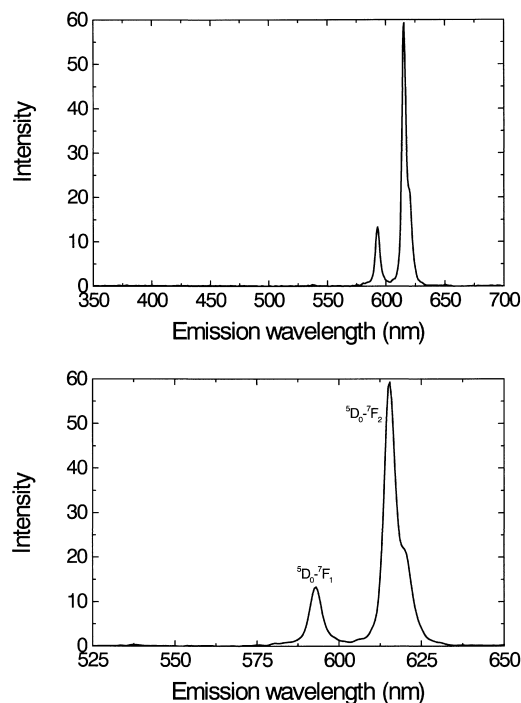


Fig. 2. Emission spectrum of Eu/La/CA mixed complex. 80% Eu<sup>3+</sup>, 20% La<sup>3+</sup>. Initial sample.

their <sup>5</sup>D<sub>0</sub>, <sup>5</sup>D<sub>1</sub>, <sup>5</sup>D<sub>2</sub>, <sup>5</sup>D<sub>3</sub> and <sup>5</sup>L<sub>6</sub> levels. The emission was measured at 616 nm, which means that all of the excited states mentioned before relax – at least partly – through the <sup>5</sup>D<sub>0</sub> level. In some Eu<sup>3+</sup> complexes a ligand-to-metal charge transfer state (CT) can be assumed, which can give a very effective relaxation way from the levels above <sup>5</sup>D<sub>2</sub> [11] especially at room temperature. The presence of <sup>7</sup>F<sub>*i*</sub>–<sup>5</sup>D<sub>*j*</sub> (*i* = 0, 1, 2, 3) and <sup>7</sup>F<sub>*i*</sub>–<sup>5</sup>L<sub>6</sub> transitions in the excitation spectra (Fig. 1) means that there is not any effective non-radiative relaxation way – e.g. ligand-to-metal CT state from the excited states above <sup>5</sup>D<sub>2</sub> level towards the ground state.

The emission spectra (Fig. 2) consist of two bands of Eu<sup>3+</sup> (<sup>5</sup>D<sub>0</sub>–<sup>7</sup>F<sub>1</sub> and <sup>5</sup>D<sub>0</sub>–<sup>7</sup>F<sub>2</sub> transitions). Let us note that the <sup>5</sup>D<sub>0</sub>–<sup>7</sup>F<sub>0</sub> transition (580 nm), which is always present in solution, has an intensity being under the detection limit. Moreover, the ligand has a broad, very weak emission band around 400 nm.

The shape and relative intensity of Eu<sup>3+</sup> emission bands does not depend on the excitation wavelength. From the higher excited states of Eu<sup>3+</sup> there are not any luminescence emission, these states relax either to the lowest lying excited state (<sup>5</sup>D<sub>0</sub>) or to the ground state (<sup>7</sup>F<sub>0</sub>) only by non-radiative transitions. (In solution the luminescence from a higher excited state can in some cases be observed [14–16].) The asymmetry in the <sup>5</sup>D<sub>0</sub>–<sup>7</sup>F<sub>*i*</sub> transitions indicate the presence of more than one emitting species. Nevertheless, the decay curves can be fitted well with a single term of exponentials (Fig. 3).

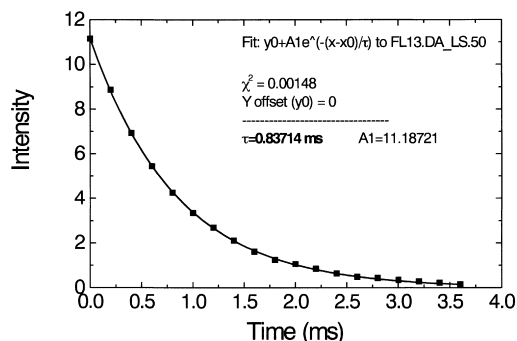


Fig. 3. Decay of  $\text{Eu}^{3+}$  luminescence.  $\lambda_{\text{ex}} = 337 \text{ nm}$ ,  $\lambda_{\text{em}} = 616 \text{ nm}$ . 70%  $\text{Eu}^{3+}$ , 30%  $\text{La}^{3+}$ . Initial sample.

### 3.2. Photochemical degradation

Irradiating the samples by UV light having wavelength of shorter than 330 nm the emission intensity (measured at 616 nm) decreases in time. It means that a photochemical degradation occurs in the irradiated samples. The wavelength of irradiating light was 240 nm and the time of irradiation was 1800 s. (It was a pulsed irradiation by flashes of 10  $\mu\text{s}$  using 50 Hz repetition rate!) In the following, the samples not treated with irradiation mentioned before will be referred to as ‘initial’.

The absolute change of photodegradation is similar in the case of low and high  $\text{Eu}^{3+}$  content. That is, the relative change is higher at low  $\text{Eu}^{3+}$  content. Fig. 4 (A) and (B) show the excitation spectra and the differences in them.

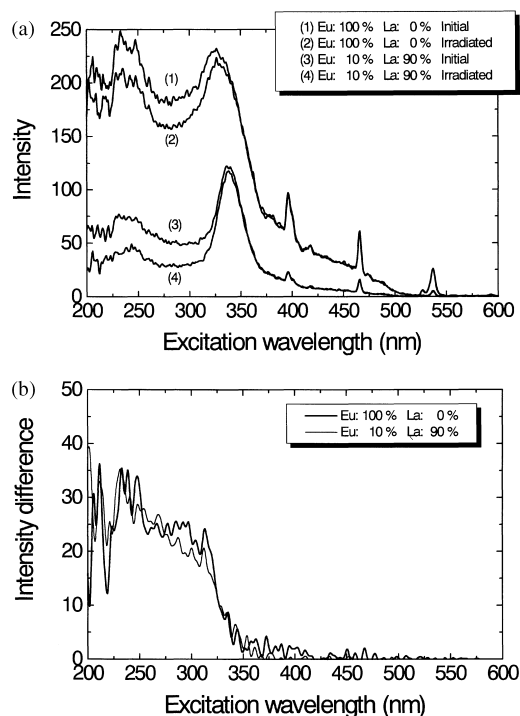


Fig. 4. (A) Excitation spectra of initial and irradiated samples. (B) Differences of excitation spectra. Initial – irradiated.  $\lambda_{\text{em}} = 616 \text{ nm}$ .

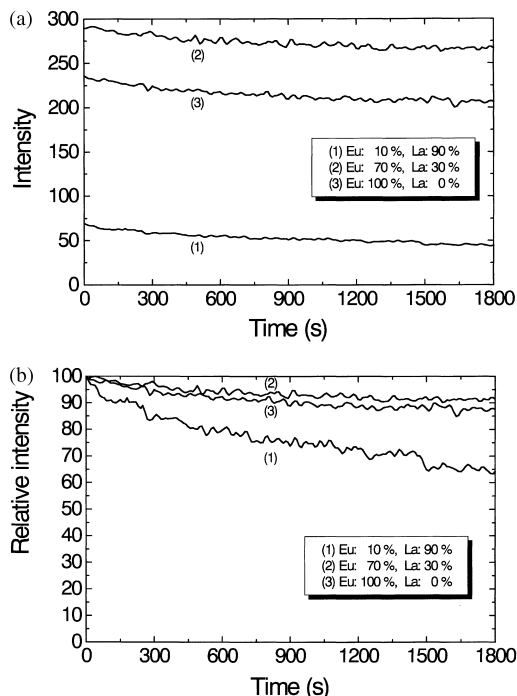


Fig. 5. Decrease of emission intensity under irradiation. (A) Measured intensity. (B) Relative intensity.  $\lambda_{\text{ex}} = 240 \text{ nm}$ ,  $\lambda_{\text{em}} = 616 \text{ nm}$ .

Fig. 5 (A) and (B) show how the photodegradation develops in time. The curves of Fig. 5 (A) and (B) are non-exponential and have a characteristic time of about 5 min. The emission intensity does not seem to tend to zero, the yield of ligand-to-metal energy transfer decreases only slightly. From the curves of emission intensity before and after irradiation (Fig. 6 (A) and (B)) it can be well seen that the samples of low  $\text{Eu}^{3+}$  content loose even more than 30% of its emission intensity. At high  $\text{Eu}^{3+}$  content this decrease is only a few percent. The independent variable of Figs. 6–10 is  $C_{\text{Eu}}$ , which stands for the number of  $\text{Eu}^{3+}$  ions among every hundreds of lanthanide ions.

Comparing the curves of Fig. 7 (A) ( $\lambda_{\text{ex}} = 337 \text{ nm}$ ) and Fig. 7 (B) ( $\lambda_{\text{ex}} = 240 \text{ nm}$ ) it can be seen clearly that the photodegradation is significant only in the case of shorter excitation wavelength. (The curves (1) and (2) of Fig. 6 (A) are displayed also in Fig. 7 (B) for a later discussion of other point of view.)

The main reason of this photodegradation effect is probably that a smaller fraction of the double-bonds of the CA ligands are cut by the short wavelength UV light having high enough energy. On the other hand, the reason, why the degree of photodegradation is higher at low  $\text{Eu}^{3+}$  concentration, is not clear yet. This effect needs further studies.

Comparing to  $\text{Eu}/\text{Gd}/\text{CA}$  [13], both the absolute and the relative degree of photodegradation are smaller in the case of  $\text{Eu}/\text{La}/\text{CA}$ . But in both of these systems the photodegradation effect is stronger at low  $\text{Eu}^{3+}$  content. Thus, it seems that the InterMET (the long-distance interaction) is affected more strongly than the IntraMET (the short-distance interaction) (see 3.3).

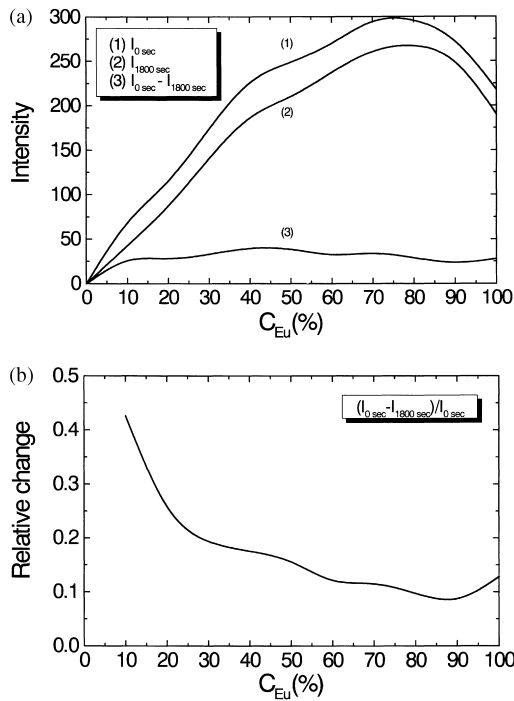


Fig. 6. (A) Emission intensity before and after irradiation. (B) Relative change of emission intensity.  $\lambda_{ex} = 240$  nm,  $\lambda_{em} = 616$  nm.

### 3.3. Sensitized luminescence of $Eu^{3+}$

As in the case of  $Eu/Gd/CA$  [13], it is shown in the following that both intramolecular energy transfer

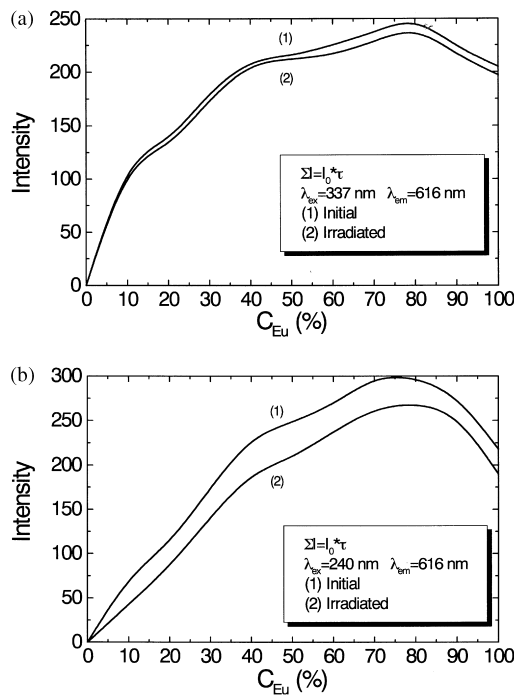


Fig. 7.  $\Sigma I = I_0 \tau$  integrated emission intensity. (A)  $\lambda_{ex} = 337$  nm. (B)  $\lambda_{ex} = 240$  nm.  $\lambda_{em} = 616$  nm in both cases.

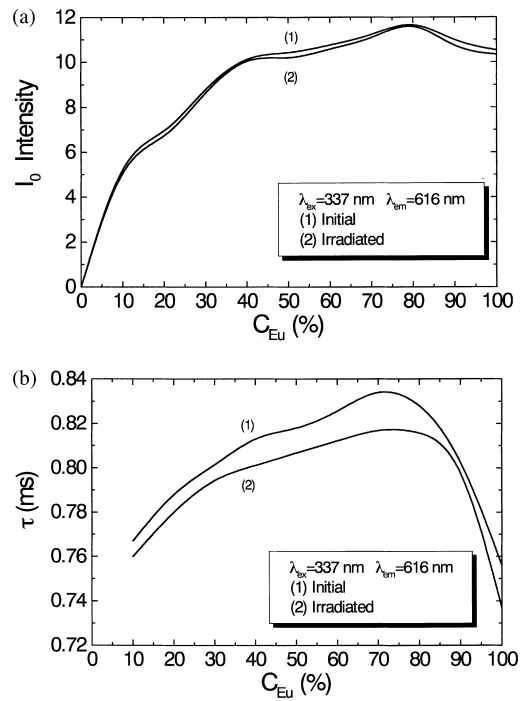


Fig. 8. (A)  $I_0$  initial intensity. (B)  $\tau$  decay time.  $\lambda_{ex} = 337$  nm.  $\lambda_{em} = 616$  nm.

(IntraMET) and intermolecular energy transfer (InterMET) have contribution to the emission of  $Eu^{3+}$ .

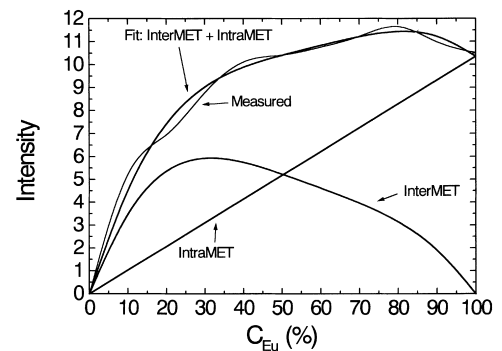


Fig. 9. Fit for measured initial intensity.  $\lambda_{ex} = 337$  nm.  $\lambda_{em} = 616$  nm.

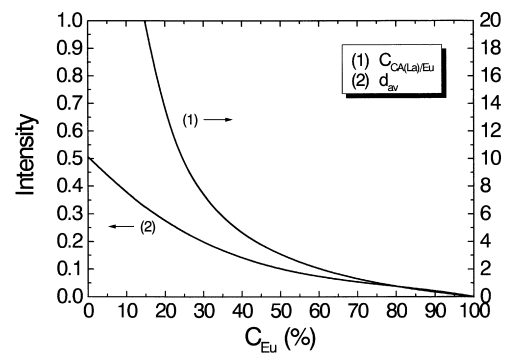


Fig. 10. (1)  $C_{CA(La)/Eu}$ : number of La-bonded CAs per  $Eu^{3+}$  ions. (2)  $d_{av}$ : factor proportional to the average distance of InterMET.

The decay of  $\text{Eu}^{3+}$  luminescence can be fitted with one-exponential:

$$I(t) = I_0 e^{(-1/\tau)} \quad (1)$$

where  $I_0$  stands for the intensity right after the excitation (initial intensity) and  $\tau$  stands for the decay time. Integrating (Eq. (1)) one gets the integrated emission intensity, the data points of measured spectra. The integrated emission intensity is equal to the product of the initial intensity and the decay time:

$$\int_0^{\infty} I(t) dt = I_0 \tau \quad (2)$$

The integrated emission intensity shows an interesting dependence on the  $\text{Eu}^{3+}$  contents of the samples (Fig. 7 (A) and (B)).

Increasing the  $\text{Eu}^{3+}$  content the emission intensity increases monotonically, but not linearly up to the ratio of about 80%  $\text{Eu}^{3+}$ /20%  $\text{La}^{3+}$ . The further increase of  $\text{Eu}^{3+}$  content results in a slight decrease in the integrated emission intensity. In the case of excitation wavelength of 337 nm the initial and irradiated samples show very similar values (Fig. 7 (A)). The difference between them is of only a few percent. In the case of excitation wavelength of 240 nm the difference in the integrated emission intensity between initial and irradiated samples is higher (Fig. 7 (B)). But all of the curves of Fig. 7 (A) and (B) show similar intensity dependence on the  $\text{Eu}^{3+}$  content of the samples.

Let us analyse the dependence of initial intensity and decay time on the  $\text{Eu}^{3+}$  content (Fig. 8 (A) and (B)), which one of them is responsible for the shape of curves of Fig. 7 (A) and (B).

From Fig. 8 (A) it can be well seen that the dependence of initial intensity is very similar to the dependence of integrated emission intensity on the  $\text{Eu}^{3+}$  content (Fig. 7 (A)). The decay time depends much less on the  $\text{Eu}^{3+}$  content (the maximum and minimum values of it differ by not more than 15%), but anyway this dependence is also significant. Thus, it can be concluded that although the initial intensity is primarily responsible for the shape of the curves of integrated emission intensities, the decay time gives also a non-negligible contribution. Both of them reach their maximum values at 70–80%  $\text{Eu}^{3+}$  content. The initial intensities are proportional to the yield of energy transfer towards  $\text{Eu}^{3+}$ . The decay times are related to the quenching processes influencing the emitting excited state of  $\text{Eu}^{3+}$ . That is, both the most efficient energy transfer and the lowest rate of quenching of  $^5\text{D}_0$  level occur at about 70–80%  $\text{Eu}^{3+}$  content.

Now, let us focus on the quantitative details of IntraMET and InterMET. Because the lifetime of  $\text{Eu}^{3+}$  is longer than the lifetime of CA by many orders of magnitude, the result of energy transfer can be seen purely on the curve of initial intensity. In the case of a initial sample it is curve (1) of Fig. 8 (A). In Fig. 9 it is also shown and is named ‘measured’. For calculation it is fitted by polynomials (curve:

‘fit’). This initial intensity of luminescence of  $\text{Eu}^{3+}$  derives from IntraMET and InterMET:

$$I_{\text{Eu}} = I_{\text{IntraMET}} + I_{\text{InterMET}} \quad (3)$$

in the case of IntraMET the energy is transferred from the CAs bonded to a  $\text{Eu}^{3+}$  (let  $C_{\text{CA}(\text{Eu})}$  stand for their number) towards that  $\text{Eu}^{3+}$ . In the case of InterMET the energy is transferred from the CAs bonded to a  $\text{La}^{3+}$  (let  $C_{\text{CA}(\text{La})}$  stands for their number) towards a  $\text{Eu}^{3+}$ . For the latter let us calculate  $C_{\text{CA}(\text{La})/\text{Eu}}$ , the number of  $\text{La}^{3+}$ -bonded CAs per  $\text{Eu}^{3+}$ :

$$C_{\text{CA}(\text{La})/\text{Eu}} = \frac{C_{\text{CA}(\text{La})}}{C_{\text{Eu}}} = \frac{C_{\text{CA}}}{C_{\text{Eu}}} - 3 \quad (4)$$

where  $C_{\text{CA}} = C_{\text{CA}(\text{Eu})} + C_{\text{CA}(\text{La})} = 300$  is the number of the CAs for every hundreds of lanthanide ions.

The luminescence intensity deriving from IntraMET (in Fig. 9 it is shown as a straight line) is supposed to be proportional to the number (or-if you like -concentration) of  $\text{Eu}^{3+}$  ions:

$$I_{\text{IntraMET}} = K_1 C_{\text{Eu}} \quad (5)$$

where  $K_1$  is a constant. The difference between the total initial luminescence intensity and the intensity deriving from IntraMET is the intensity deriving from InterMET. It is also shown in the Fig. 9. Because the  $\text{Eu}^{3+}$  ions are the final emitters let us write  $I_{\text{InterMET}}$  as a product of  $C_{\text{Eu}}$  and an other factor  $d_{\text{av}}$ :

$$I_{\text{InterMET}} = C_{\text{Eu}} d_{\text{av}} \quad (6)$$

the curve of  $d_{\text{av}}$  is shown in Fig. 10.  $d_{\text{av}}$  is the highest when the concentration of  $\text{Eu}^{3+}$  tends to zero. Increasing  $C_{\text{Eu}}$  the value of  $d_{\text{av}}$  decreases monotonically. It is because the  $\text{Eu}^{3+}$  ions compete each other, and at higher concentration of  $\text{Eu}^{3+}$  the InterMET is effective only the from La-bonded CAs being in the closest proximity of the  $\text{Eu}^{3+}$  complex. Thus,  $d_{\text{av}}$  is proportional to the average distance of InterMET. Because the exact types and roles of possible InterMET processes are not yet known, it cannot be concluded any quantitative meaning to the polynomial fit describing the shape of  $d_{\text{av}}$ :

$$d_{\text{av}} = 0.4615 - 0.0119 C_{\text{Eu}} + 12 \cdot 10^{-4} C_{\text{Eu}}^2 - 4.853 \cdot 10^{-7} C_{\text{Eu}}^3 \quad (7)$$

Now let us compare the shape of curves of  $d_{\text{av}}$  and  $C_{\text{CA}(\text{La})/\text{Eu}}$  (Fig. 10). It can be seen that in the case of  $C_{\text{Eu}} > 70\%$  the two curves goes quite together. At lower concentration of  $\text{Eu}^{3+}$   $C_{\text{CA}(\text{La})/\text{Eu}}$  (which is the number of La-bonded CAs per  $\text{Eu}^{3+}$  ions) tends to the infinity but  $d_{\text{av}}$  tends to a finite number. That is the CAs being farther and farther from a  $\text{Eu}^{3+}$  ion can transfer their energy towards a  $\text{Eu}^{3+}$  ion by drastically less and less efficiency.

The most possible types of InterMET can be dipole–dipole, dipole–quadrupole interactions and energy migration. To distinguish between them quantitatively needs further studies.

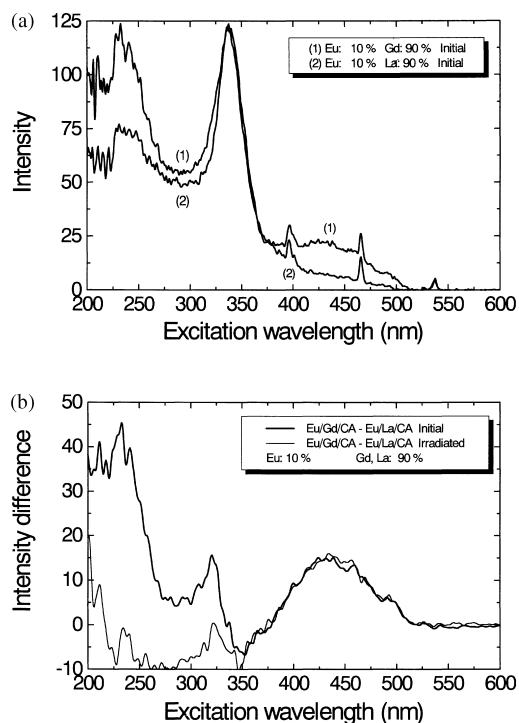


Fig. 11. (A) Excitation spectra of Eu/La/CA and Eu/Gd/CA mixed complexes.  $\lambda_{em} = 616$  nm. 10%  $\text{Eu}^{3+}$ , 90%  $\text{La}^{3+}$  or  $\text{Gd}^{3+}$ . Initial samples. (B) Differences of excitation spectra.

Finally, let us compare the excitation spectra of Eu/La/CA and Eu/Gd/CA systems (Fig. 11 (A)). In both of them the ligand bands and the lines of  $\text{Eu}^{3+}$  can be well identified. Significant differences belong to the shorter wavelength ligand band (centered at 240 nm) and between 380 nm and 520 nm. The qualitative picture is the same at higher  $\text{Eu}^{3+}$  concentration. Because the excitation conditions of these powders were the same, these differences in the excitation spectra should mean: (a) different absorption coefficient – it is possible in the case of the band centred at 440 nm (non-monomer forms of complexes); (b) different yield of energy transfer towards  $\text{Eu}^{3+}$  – it is likely the situation at the band of 240 nm. Because the decay time of Eu/La/CA and Eu/Gd/CA systems is nearly the same and the  $I_0$  initial intensity is different, it means – see Eq. (2) – that in the Eu/La/CA system the yield of energy transfer is a bit lower than in Eu/Gd/CA. After the irradiation (which causes the photodegradation) the difference between the two systems mentioned became lower in the case of band at 240 nm, but remains unchangeable over 380 nm (Fig. 11(B)). This fact also means that the exciting photons having not high enough energy can not influence the chemical bonds of the samples.

#### 4. Conclusions

The Eu/La/CA complex is a promising light-converting material. The photoemission of it occurs in 99% at the two

main emission lines of  $\text{Eu}^{3+}$  (592 nm, 616 nm). From all of the ligand states and the higher-lying excited states of  $\text{Eu}^{3+}$  there is effective energy transfer towards the  $^5\text{D}_0$  level. The integrated emission intensity of mixed complexes depends on the ratio of  $\text{Eu}^{3+}/\text{La}^{3+}$  contents. Both the maximal emission intensity and the lowest rate of quenching of the  $^5\text{D}_0$  level were found to be between 70–80%  $\text{Eu}^{3+}$  content. It means that the energy transfer is the most efficient when the CA/ $\text{Eu}^{3+}$  ratio of the solid sample is about 3.8 : 1 (which is higher than the stoichiometric 3 : 1 of  $\text{Eu}^{3+}/(\text{CA})_3$ ).

The energy transfer consists of IntraMET and InterMET processes. The IntraMET can be supposed to be proportional to the concentration of  $\text{Eu}^{3+}$ . The luminescence intensity deriving from InterMET can be written as a product of the concentration of  $\text{Eu}^{3+}$  and a factor which is proportional to the average distance of InterMET. The lower the  $C_{\text{Eu}}$ , the higher is the  $d_{av}$ . Nevertheless, the efficiency of InterMET from longer distances decreases drastically.

The samples show some photochemical degradation under UV irradiation of short wavelength. It is significant at low  $\text{Eu}^{3+}$  contents.

The effects found seem to be worth further studying: (a) at different temperature; (b) with higher spectral resolution and (c) with better time resolution (on the ns time scale).

#### Acknowledgements

This work was supported by the National Science and Research Foundation of Hungary under Contract No. OTKA-7621.

#### References

- [1] S.I. Weissman, *J. Chem. Phys.* 10 (1942) 214.
- [2] J.C.G. Bünzli, in: J.C.G. Bünzli, G.R. Choppin (Eds.), *Lanthanide Probes in Life, Chemical and Earth Sciences, Theory and Practice*, Elsevier, Amsterdam, 1989, p. 219.
- [3] M. Elbanowski, B. Makowska, *J. Photochem. Photobiol. A: Chem.* 99 (1996) 85.
- [4] I. Hemmilä, *J. Alloys Compounds* 225 (1995) 480.
- [5] E. Soini, *Trends Anal. Chem.* 9 (1990) 90.
- [6] C. de M. Donegá, S.A. Junior, G.F. de Sá, *Chem. Commun.* (1996) 1199.
- [7] J.C.G. Bünzli, E. Moret, V. Foiret, K.J. Schenk, W. Mingzhao, J. Linpei, *J. Alloys Compounds* 207/208 (1994) 107.
- [8] P.A. Tanner, Y.L. Liu, M. Chua, and M.F. Reid, *J. Alloys Compounds* 207–208 (1994) 83.
- [9] J. Erostyák, A. Buzády, A. Kaszás, L. Kozma, I. Hornyák, *J. Lumin.* 72–74 (1997) 570.
- [10] J. Li, G. Shen, J. Hu, Y. Zeng, *Fresenius J. Anal. Chem.* 342 (1992) 552.
- [11] M.T. Berry, P.S. May, H. Xu, *J. Phys. Chem.* 100 (1996) 9216.
- [12] J.C.G. Bünzli, E. Moret, V. Foiret, K.J. Schenk, W. Mingzhao, J. Linpei, *J. Alloys Compounds*, 207/208 (1994) 107.
- [13] J. Erostyák, A. Buzády, I. Hornyák, L. Kozma, *J. Photochem. Photobiol. A: Chem.* 115 (1998) 21.
- [14] J. Erostyák, A. Buzády, L. Kozma, I. Hornyák, *Spectrosc. Lett.* 28(3) (1995) 473.
- [15] J. Georges, *Analyst* 118 (1993) 1481.
- [16] J.V. Beitz, *J. Alloys Compounds* 207/208 (1994) 41.